JOURNAL OF SOLID STATE CHEMISTRY 94, 352–361 (1991)

Single-Crystal X-Ray and Neutron Diffraction Investigations of the Temperature Dependence of the Structure of the T_c = 10 K Organic Superconductor κ-$(ET)_2Cu(NCS)_2$

ARTHUR J. SCHULTZ, MARK A. BENO, URS GEISER, H. HAU WANG, ARAVINDA M. KINI, AND JACK M. WILLIAMS

Chemistry and Materials Science Divisions, Argonne National Laboratory, Argonne, Illinois 60439

AND MYUNG-HWAN WHANGBO

Department of Chemistry, North Carolina State University, Raleigh, North Carolina 27695

Received March 29, 1991; in revised form June 10, 1991

The crystal structure of κ-$(ET)_2Cu(NCS)_2$ [ET or BEDT-TTF = bis(ethylenedithio)tetrathiafulvalene, $C_{10}H_8S_8$] has been examined by single-crystal neutron and X-ray diffraction at temperatures between 298 and 15 K. Comparison of the low temperature ordered structures determined by use of X-ray and neutron diffraction with the previously reported crystallographically disordered room temperature X-ray structure indicates the avoidance of close H···H contacts as the reason for the conformational disorder of the terminal ethylene groups of the ET molecules at high temperatures. The space group is monoclinic noncentrosymmetric $P2_1$, $Z = 2$. Unit cell parameters at 118 K are $a = 16.359(4)$, $b = 8.418(2)$, $c = 12.855(3)$ Å, $\beta = 111.21(2)°$, and $V = 1650.3(7)$ Å^3; at 15 K, $a = 16.373(5)$, $b = 8.375(3)$, $c = 12.775(6)$ Å, $\beta = 111.45(4)°$, and $V = 1630(1)$ Å^3. The interlayer spacing $a \cdot \sin\beta$ remains constant upon cooling from 298 to 15 K even though the a axis increases slightly in length.

Introduction

The organic superconductor κ-$(ET)_2Cu(NCS)_2$ [ET or BEDT-TFF = bis(ethylenedithio)tetrathiafulvalene, $C_{10}H_8S_8$] has a superconducting critical temperature, T_c, of 10.4 K (*1–3*) and the largest known negative pressure dependence of T_c (-3 K/kbar) (*4*). Upon cooling, the sample resistivity at first indicates metallic behavior, followed by rising resistivity with a maximum at ~90 K, after which the resistivity drops and becomes zero at ~10 K (*1*). A previous study of the single-crystal X-ray diffraction structures at 298 and 104 K reported conformational ordering of the terminal ethylene (—CH_2—CH_2—) groups of the ET molecules at the lower temperature compared to a disordered structure at room temperature (*5*). A similar ethylene group conformational ordering in β-$(ET)_2I_3$ (T_c = 1.5 K,

0022-4596/91 $3.00

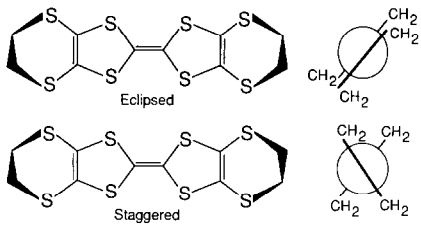

FIG. 1. Schematic view of the two possible ethylene group arrangements of ET where the C–S and C–C bonds of the ethylenedithio units (–S–CH_2–CH_2–S–) are represented by wedges to distinguish the C atoms lying above and below the molecular π-framework. The diagram on the right of each molecule depicts the eclipsed and staggered arrangements of the ethylene groups when viewed parallel to the central C=C double bond.

ambient pressure) under mild pressure (0.5 kbar) results in a large jump in T_c to ~8 K (*6*). In all the cases of ET conformational disorder, one of the ethylene groups is ordered while the other ethylene group exhibits random disorder such that, when viewed along the central C=C double bond, the two groups are either eclipsed or staggered relative to each other (Fig. 1). More recently, weak X-ray diffuse scattering indicative of a short range modulation of the average crystal structure of κ-(ET)$_2$Cu(NCS)$_2$ was observed at 23 K (*7*). In this paper we report the results of the first neutron diffraction study κ-(ET)$_2$Cu(NCS)$_2$ at 15 K, the lowest temperature achieved in any reported full structural study of this material. Variable temperature X-ray diffraction results are also reported. We have used these results to examine in detail the H···anion and H···donor contacts in order to provide an understanding of the disorder-to-order transition that occurs upon cooling.

Experimental

X-Ray Diffraction

Single crystals were grown by use of electrocrystallization techniques (*3*). Broadening and splitting of some of the Bragg peaks below at least 150 K were observed with one crystal, which was cooled by use of a closed-cycle helium refrigerator on a Huber four-circle goniostat in one experiment and with a nitrogen gas flow cooling apparatus on a Nicolet P3/F diffractometer in another. However, after several cooling and warming cycles this effect was not reproducible and only gradual changes in the lattice parameters (Fig. 2), and virtually no change in the peak profile widths, were observed to temperatures as low as 113 K. No evidence of peak broadening was obtained from several other crystals which were examined.

A complete data set at 118 K was obtained for comparison to the room temperature X-ray structure (*3*) and to the 15 K neutron diffraction structure obtained by the study described below. The X-ray data were obtained on a Syntex $P2_1$ four-circle diffractometer equipped with a nitrogen gas flow cooling system. Data collection and refinement parameters are listed in Table I. In the final cycles of least-squares refinements, anomalous scattering was included and all nonhydrogen atoms were refined with anisotropic thermal parameters (*8*). The atomic positional and equivalent isotropic thermal parameters are given in Table II. Since the

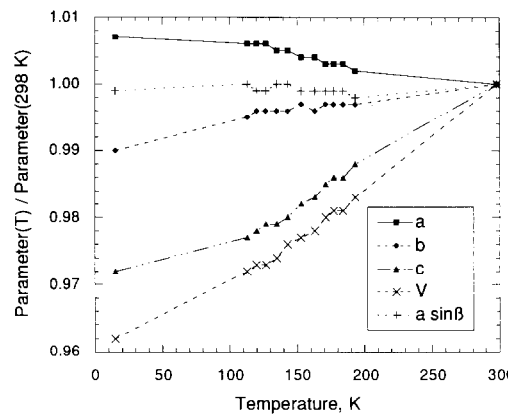

FIG. 2. Temperature dependence of the unit cell parameters between 15 K and room temperature. The 15 K data points were derived from neutron diffraction data. All other data points are based on X-ray data.

TABLE I

UNIT CELL, DATA COLLECTION, AND REFINEMENT PARAMETERS FOR κ-$(ET)_2Cu(NCS)_2$

	Space group: monoclinic $P2_1$ $Z = 2$	
	15 K	118 K
a(Å)	16.373(5)	16.359(4)
b(Å)	8.375(3)	8.418(2)
c(Å)	12.775(6)	12.855(3)
β(deg.)	111.45(4)	111.21(2)
V(Å^3)	1630(1)	1650.3(7)
Radiation	Neutrons	X-rays
Wavelength(s)	λ = 0.9–4.2 Å determined by time-of-flight	Mo$K\alpha$, λ = 0.7107 Å
Data collection technique	Time-of-flight Laue with 30 × 30 cm^2 position-sensitive area detector	θ–2θ scans
Abs. coefficient μ(cm^{-1})	0.681 at λ = 0.7 Å 2.046 at λ = 4.2 Å	17.4
Abs. correction	Spherical, r = 0.062 cm	Polyhedral
No. of reflections in final l.s.	1125 ($F^2 > 3\sigma$, no overlap from twin)	4339 ($F > 3\sigma$)
Function minimized	$\Sigma w(F_o^2 - F_c^2)^2$	$\Sigma w(\|F_o\| - \|F_c\|)^2$
$R(F)$	0.063	0.040
$R_w(F)$		0.035
$R_w(F^2)$	0.120	
GOF	1.37	1.35

Note. For comparison, unit cell parameters at 298 K (Ref. (3)) are a = 16.256(3), b = 8.456(1), c = 13.143(3) Å, β = 110.28(1)°, and V = 1694.8(6) Å^3.

coordinates for the X-ray structures determined at 295 and 104 K by Urayama *et al.* (*5*) have not been published, a direct comparison with the results in this study is not possible.

Neutron Diffraction

Many large crystals weighing from 0.5 to several milligrams were examined on the time-of-flight single crystal diffractometer (SCD) at the Argonne Intense Pulsed Neutron Source (*9*). The instrument is equipped with a position-sensitive area detector, which, in combination with the spectral range of neutron wavelengths available from the source, provides the ability to sample a large volume of reciprocal space with a single goniostat setting. Using these capabilities, it was quickly determined that all of the large crystals were twinned on their [1,0,0]/[$\bar{1}$,0,0] faces such that $hk0$ reflections from one twin, and $\bar{h}k0$ reflections from the second twin, are coincident.

The largest untwinned single crystal weighed 0.41 mg, which is generally an unsuitable sample size for a complete neutron diffraction structural analysis on the SCD. However, partial sets of data were obtained at temperatures of 298, 150, 80, and 20 K from the 0.41-mg single crystal and from a 3.6-mg twinned crystal. In both cases, there was no variation of peak widths with temperature. A complete unique quadrant of data was then obtained at 15 K by use of the 3.6-mg crystal in a manner previously described (*10*). The data were corrected for the Lorentz factor, the incident spectrum, the detector efficiency, dead-time losses, and crystal absorption. Because of the twinning problem, a large portion of the data were not useable due to partially overlap-

TABLE II

ATOMIC COORDINATES AND EQUIVALENT ISOTROPIC THERMAL PARAMETERS FOR κ-$(ET)_2Cu(NCS)_2$ AT 118 K DERIVED FROM X-RAY DIFFRACTION DATA

Atom	x	y	z	U_{eq}[a]
Cu	0.00027(4)	0.3585	0.33816(6)	0.0229(2)
S(21)	−0.0097(1)	−0.0039(2)	0.0603(1)	0.0303(5)
S(22)	−0.02104(9)	0.1255(2)	0.6610(1)	0.0250(4)
N(21)	−0.0016(3)	0.2373(6)	0.2121(4)	0.027(2)
N(22)	−0.0121(3)	0.2582(7)	0.4648(4)	0.026(2)
C(21)	−0.0052(3)	0.1378(7)	0.1473(4)	0.024(2)
C(22)	−0.0156(3)	0.1986(7)	0.5441(4)	0.018(2)
S(1)	0.54484(8)	0.0743(2)	0.2433(1)	0.0180(4)
S(2)	0.62834(8)	−0.1687(2)	0.4141(1)	0.0174(4)
S(3)	0.37905(8)	0.0867(2)	0.3130(1)	0.0171(4)
S(4)	0.44764(8)	−0.1740(2)	0.4744(1)	0.0184(4)
S(5)	0.69786(9)	0.1346(2)	0.1833(1)	0.0223(5)
S(6)	0.80369(9)	−0.1356(3)	0.3995(1)	0.0299(5)
S(7)	0.21027(8)	0.1169(2)	0.3432(1)	0.0205(4)
S(8)	0.2881(1)	−0.2038(2)	0.5296(1)	0.0350(6)
C(1)	0.5371(3)	−0.0465(7)	0.3484(4)	0.016(2)
C(2)	0.4631(3)	−0.0478(7)	0.3751(4)	0.014(2)
C(3)	0.6551(3)	0.0290(7)	0.2686(4)	0.017(2)
C(4)	0.6934(3)	−0.0779(7)	0.3479(4)	0.017(2)
C(5)	0.3106(3)	0.0172(8)	0.3805(4)	0.018(2)
C(6)	0.3418(3)	−0.1034(8)	0.4531(4)	0.022(2)
C(7s)	0.8127(4)	0.084(1)	0.2407(6)	0.049(3)
C(8s)	0.8349(4)	−0.076(1)	0.2855(6)	0.045(3)
C(9)	0.1523(3)	0.0072(8)	0.4159(4)	0.021(2)
C(10)	0.2114(4)	−0.0506(8)	0.5322(5)	0.026(2)
S(11)	0.44093(8)	0.2976(2)	0.9747(1)	0.0172(4)
S(12)	0.37458(9)	0.0319(2)	0.8183(1)	0.0182(4)
S(13)	0.61977(8)	0.2967(2)	0.9131(1)	0.0156(4)
S(14)	0.54113(9)	0.0453(2)	0.7484(1)	0.0185(4)
S(15)	0.2822(1)	0.3269(2)	1.0315(1)	0.0329(5)
S(16)	0.20778(9)	−0.0042(2)	0.8543(1)	0.0217(4)
S(17)	0.79594(9)	0.2725(2)	0.9026(1)	0.0245(5)
S(18)	0.69759(9)	−0.0144(2)	0.6941(1)	0.0240(5)
C(11)	0.4579(3)	0.1727(7)	0.8776(4)	0.016(2)
C(12)	0.5305(3)	0.1750(7)	0.8495(4)	0.015(2)
C(13)	0.3363(3)	0.2260(7)	0.9569(4)	0.017(2)
C(14)	0.3062(3)	0.1016(7)	0.8862(4)	0.016(2)
C(15)	0.6869(3)	0.2082(7)	0.8509(4)	0.017(2)
C(16)	0.6500(3)	0.0959(7)	0.7726(4)	0.018(2)
C(17s)	0.2037(4)	0.1768(7)	1.0357(4)	0.022(2)
C(18s)	0.1475(3)	0.1166(8)	0.9205(4)	0.020(2)
C(19)	0.8336(4)	0.2034(8)	0.7964(5)	0.023(2)
C(20)	0.8133(4)	0.0283(8)	0.7681(5)	0.029(2)

[a] $U_{eq} = \frac{1}{3}\sum_{ij} U_{ij} a_i^* a_j^* \mathbf{a}_i \cdot \mathbf{a}_j$.

ping diffraction peaks that could not be resolved for obtaining single-peak integrated intensities. Overlapping peaks were identified by calculating the predicted peak positions from the orientation matrices of each twin. Since the *hk*0 reflections from one twin exactly overlap with the equivalent $\overline{hk}0$ reflections from the other twin, these reflections were included in the refinements with a separate scale factor.

Least-squares refinements, using a multiwavelength program based on ORFLS (*11*), of the atom positional coordinates and isotropic thermal parameters of all 59 atoms, including the 16 hydrogen atoms, converged with $R(F) = 0.068$ and $R_w(F^2) = 0.133$ but with nonpositive-definite thermal parameters for 15 atoms, mostly sulfur atoms on one ET molecule and carbon atoms on the other ET. It was observed that high correlations existed between parameters of the atoms of the two independent ET molecules, apparently due to the nearly $P2_1/c$ symmetry of the ET molecule packing. Therefore, the positional and thermal parameters of one ET molecule were made dependent on the other after an appropriate origin shift. However, the *R*-factors doubled and six of the independent ET atoms remained nonpositive-definite. In the final refinement, which included an isotropic extinction correction (*12*), the positional parameters of all atoms were varied but the isotropic thermal parameters of 11 atoms were fixed with $B = 0.1$ Å^2 (Table III). The nonpositive-definite temperature factors are due to the effects of the twinning which limited the $(\sin\theta)/\lambda$ range of nonoverlapping Bragg peaks. However, the positional parameters appear to be correct since the structure is reasonable and entirely consistent with that derived from the previous X-ray analyses.

Results and Discussion

Based on our neutron and X-ray diffraction measurements, under most ordinary cooling conditions there does not appear to be any observable low temperature structural phase transition in κ-$(ET)_2Cu(NCS)_2$ that could explain the peak at 90 K in the resistivity. The peak broadening and splitting observed for one crystal by use of X-rays was not reproduced with other crystals. The very weak diffuse scattering arising from stacking faults reported by Ravy *et al.* (*7*) were obtained with a high-intensity rotating anode X-ray source and are not observable in our experiments.

As previously reported by Urayama *et al.* (*5*), cooling a crystal of κ-$(ET)_2Cu(NCS)_2$ from room temperature to ~100 K eliminates the conformational disorder of the terminal ethylene groups of the ET molecules. We have extended the temperature range of the structural studies down to 15 K by use of neutron diffraction and find that the average structure is qualitatively unchanged in comparison to those determined at ~100 K. However, the neutron data at 15 K allows us to uniquely determine the H-atom locations and to analyze the intermolecular hydrogen contacts at very low temperature, and compare them to those at higher temperatures.

The organic donor layer consists of face-to-face ET molecule dimers oriented at right angles with respect to their neighbors (Fig. 3), which is the common structural feature of κ-phase materials. In κ-$(ET)_2Cu(NCS)_2$, both ET molecules in the dimer are crystallographically independent. The layer of ET molecule dimers lies between layers formed by the planar and polymeric $Cu(NCS)_2^-$ anion (Fig. 3). At room temperature, each ET molecule assumes a random orientation with either an eclipsed or a staggered conformation of their ethylene groups, while at low temperatures the staggered conformation is adopted in both (Fig. 4). Shown in Fig. 5 are the C—H···H and C—H···anion contacts for the eclipsed and the staggered ET molecule conformations.

We have previously examined the effects of structural strain due to intermolecular contact distances that are shorter than the

TABLE III

POSITIONAL AND ISOTROPIC THERMAL PARAMETERS FOR κ-$(ET)_2Cu(NCS)_2$ AT 15 K DERIVED FROM NEUTRON DIFFRACTION DATA

Atoms	x	y	z	$U(Å^2)^a$
Cu	−0.0002(7)	0.3585	0.3360(8)	0.009(2)
S(21)	−0.008(2)	−0.012(3)	0.051(2)	0.008(5)
S(22)	−0.017(2)	0.123(4)	0.665(2)	0.014(6)
N(21)	0.0000(5)	0.235(2)	0.2098(6)	0.008(2)
N(22)	−0.0127(5)	0.252(1)	0.4624(5)	0.007(2)
C(21)	−0.0068(9)	0.130(2)	0.1458(9)	0.011(3)
C(22)	−0.0166(7)	0.189(2)	0.5442(8)	0.00127[b]
S(1)	0.544(2)	0.068(4)	0.246(2)	0.002(6)
S(2)	0.630(2)	−0.174(3)	0.416(2)	0.00127[b]
S(3)	0.383(2)	0.086(3)	0.316(2)	0.00127[b]
S(4)	0.452(2)	−0.174(3)	0.477(2)	0.003(6)
S(5)	0.698(2)	0.134(4)	0.182(2)	0.006(5)
S(6)	0.803(2)	−0.134(3)	0.401(2)	0.00127[b]
S(7)	0.211(2)	0.100(3)	0.345(2)	0.00127[b]
S(8)	0.290(2)	−0.199(3)	0.535(2)	0.00127[b]
C(1)	0.5383(9)	−0.051(2)	0.350(1)	0.012(3)
C(2)	0.4622(8)	−0.056(2)	0.3764(9)	0.00127[b]
C(3)	0.657(1)	0.022(2)	0.268(1)	0.005(3)
C(4)	0.6951(9)	−0.081(2)	0.350(1)	0.007(3)
C(5)	0.3102(9)	0.013(2)	0.3796(9)	0.001(3)
C(6)	0.3424(9)	−0.109(2)	0.4548(9)	0.003(3)
C(7s)	0.8155(9)	0.083(2)	0.2459(9)	0.005(3)
C(8s)	0.836(1)	−0.086(2)	0.286(1)	0.009(3)
C(9)	0.1507(9)	−0.003(2)	0.413(1)	0.003(3)
C(10)	0.2111(9)	−0.051(2)	0.532(1)	0.002(3)
S(11)	0.543(2)	0.042(4)	0.750(2)	0.007(7)
S(12)	0.619(2)	0.292(3)	0.914(2)	0.00127
S(13)	0.373(2)	0.024(3)	0.816(2)	0.001(5)
S(14)	0.440(2)	0.303(3)	0.974(2)	0.005(6)
S(15)	0.699(2)	−0.021(4)	0.692(2)	0.00127[b]
S(16)	0.801(2)	0.278(3)	0.904(2)	0.008(6)
S(17)	0.208(2)	−0.009(3)	0.847(2)	0.00127[b]
S(18)	0.282(2)	0.330(3)	1.025(2)	0.00127[b]
C(11)	0.5302(8)	0.171(2)	0.8496(9)	0.001(3)
C(12)	0.4574(9)	0.165(2)	0.879(1)	0.007(2)
C(13)	0.6494(9)	0.090(2)	0.7722(9)	0.000(3)
C(14)	0.6871(8)	0.207(2)	0.8539(9)	0.002(2)
C(15)	0.3042(9)	0.097(2)	0.8859(9)	0.004(3)
C(16)	0.3340(8)	0.225(2)	0.9544(8)	0.002(2)
C(17s)	0.812(1)	0.025(2)	0.768(1)	0.007(3)
C(18s)	0.8309(9)	0.202(2)	0.792(1)	0.006(3)
C(19)	0.148(1)	0.106(2)	0.921(1)	0.004(3)
C(20)	0.2025(9)	0.177(2)	1.035(1)	0.006(3)
H(7As)	0.847(2)	0.171(3)	0.315(2)	0.016(5)
H(7Bs)	0.834(2)	0.099(3)	0.170(2)	0.026(6)
H(8As)	0.796(2)	−0.169(4)	0.210(2)	0.028(7)
H(8Bs)	0.905(2)	−0.104(4)	0.315(2)	0.030(7)
H(9A)	0.116(2)	−0.087(3)	0.361(2)	0.013(6)
H(9B)	0.097(2)	0.086(3)	0.413(2)	0.016(5)

TABLE III—*Continued*

Atoms	x	y	z	$U(Å^2)^a$
H(10A)	0.244(2)	0.043(4)	0.579(2)	0.025(7)
H(10B)	0.167(2)	−0.110(3)	0.570(2)	0.009(5)
H(17As)	0.838(2)	−0.048(3)	0.849(2)	0.016(5)
H(17Bs)	0.845(2)	−0.015(3)	0.708(2)	0.014(5)
H(18As)	0.809(2)	0.279(4)	0.725(2)	0.021(6)
H(18Bs)	0.904(2)	0.221(3)	0.830(2)	0.018(5)
H(19A)	0.110(2)	0.216(4)	0.864(3)	0.037(8)
H(19B)	0.104(2)	0.019(3)	0.938(2)	0.016(6)
H(20A)	0.241(2)	0.078(4)	1.091(2)	0.022(6)
H(20B)	0.161(2)	0.233(5)	1.073(3)	0.038(8)

[a] Isotropic temperature factor of the form $\exp(-B \sin^2\theta/\lambda^2)$, where $B = 8\pi^2 U$.

[b] Temperature factor became nonpositive-definite and was set to $B = 0.1$ and not refined in the final least-squares cycles.

van der Waals radii sums (*6, 13–16*). From those studies it appears that softer intermolecular phonons, which lead to higher T_c's, are associated with structures containing C—H···donor and C—H···anion contact distances that are longer than those of materials with shorter contact distances and lower T_c's. Listed in Table IV are the short C—H···anion and C—H···donor contacts in κ-$(ET)_2Cu(NCS)_2$ which are less than or equal to the sum of the van der Waals radii (H···S = 3.00, H···C = 2.85, H···N = 2.75, H···H = 2.40 Å) at any of the three temperatures which were studied. Examination of the room temperature intradimer C—H···H contacts (Table IVc) reveals that the shortest contacts are those involving the staggered conformation (H(8As)···H(19A) = 2.13, H(9A)···H(18As) = 2.04 Å). Based on this information alone, one might predict the adoption of the eclipsed conformation at low temperature in order to avoid the shorter contact distances. However, the staggered conformation is the one that is adopted. As shown in Table IVc, one reason the staggered conformation can be accommodated at low temperature is that the two shortest H···H contacts actually *increase* in length by 0.13 and 0.21 Å, respectively, from 298 to 15 K. This unexpected result indicates a

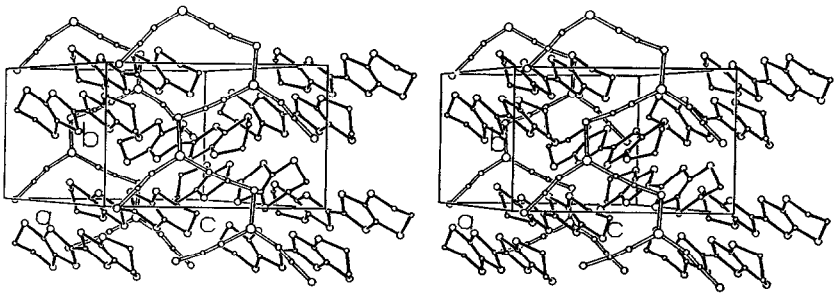

FIG. 3. Stereoview of the unit cell at 15 K derived from neutron diffraction data. Hydrogen atoms have been omitted for clarity. Ellipsoids are shown with arbitrary sizes.

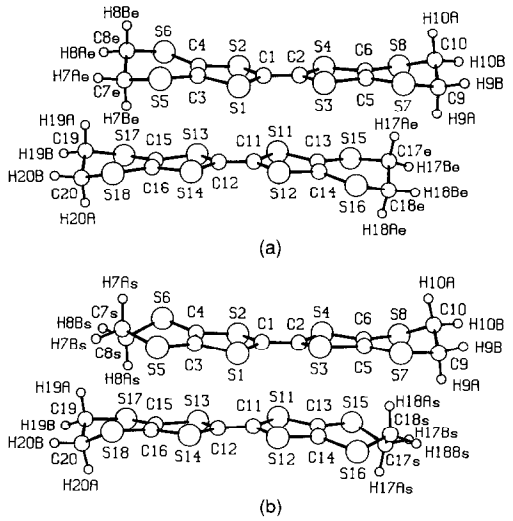

FIG. 4. The ET dimers at (a) 298 K with eclipsed conformations and at (b) 15 K with staggered conformations. At 298 K, the structure is disordered and both eclipsed and staggered conformations occur randomly. The thermal ellipsoids are shown with arbitrary sizes for clarity.

preference for the staggered conformation although at room temperature disorder occurs as a means to partially avoid the short H···H contacts.

How do these contact distances increase, with decreasing temperature, while the unit cell volume decreases due to thermal contraction? In fact, as shown in Fig. 2, only the *b* and *c* axes contract while the *a* axis *increases* slightly in length upon cooling from 298 to 15 K. Since the *a* axis has a large interlayer spacing component, it may be possible to account for the increasing lengths of the H···H contacts if the ET molecules slip in opposite directions parallel to the C(1)—C(2) and the C(11)—C(12) vectors as the anion layer separation increases. However, this is not the case since, as depicted in Fig. 6, due to a slight increase in the angle β upon cooling, the interlayer spacing $a \cdot \sin \beta$ actually remains constant for all temperatures.

Therefore, it is not possible to point to any single structural parameter as the reason for the lengthening H···H contacts. From the data in Table IV, it is seen that the contacts between H(8As) and C(15), C(16), S(17), and S(18) decrease upon cooling, as do the contacts of H(18As) with C(5), C(6), S(7), and S(8) (see Fig. 4). In the case of H(18As), the changes are greater due to longer distances initially at room temperature. For these hydrogen-to-nonhydrogen contact distances to decrease while the H···H contact distances increase requires small conformational and/or translational alterations that are not easy to evaluate with statistical certainty from the data obtained in these studies.

The one short *interdimer* H···H contact

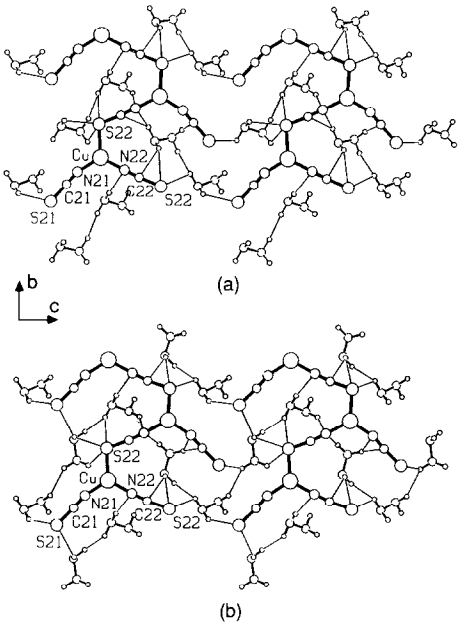

FIG. 5. The $Cu(NCS)_2^-$ anion layer with the ethylene groups from the ET donor molecules below the layer. Short H···anion and H···H contacts approximately equal to or less than the van der Waals radii sums (H···S = 3.00, H···C = 2.85, H···H = 2.40 Å) are shown as thin lines. (a) From the 298 K X-ray data with both ET molecules in the eclipsed conformation. (b) From the 15 K neutron data where the ET molecules are staggered.

TABLE IV

H···Anion and H···Donor Molecule Contact Distances[a]

Atoms[b]	15 K[c]	118 K[c]	298 K[d]	Δ(298-15)
(a) H···anion atom contact distances (Å)				
H(7Ae)–C(21)			2.67	0.00
H(7As)–N(22)	2.50	2.59	2.70	0.20
H(7Bs)–N(21)	2.67	2.73	2.66	−0.01
H(7Bs)–C(21)	2.66	2.71	2.60	−0.06
H(8Ae)–C(22)			2.80	
H(8Be)–N(22)			2.44	
H(8Be)–C(22)			2.78	
H(8Bs)–S(22)	2.85	3.01	2.86	0.01
H(8Bs)–C(22)	2.69	2.73	2.78	0.09
H(9A)–S(22)	2.74	2.81	2.93	0.19
H(9B)–N(22)	2.56	2.56	2.65	0.09
H(10B)–N(22)	2.74	2.73	2.72	−0.02
H(17As)–S(21)	2.96	3.01	3.27	0.31
H(17Be)–S(22)			2.85	
H(17Bs)–S(22)	2.78	272	2.80	0.02
H(18Ae)–S(21)			2.91	
H(18Be)–S(22)			2.85	
H(18Bs)–S(21)	2.98	2.95	2.95	−0.03
H(18Bs)–S(22)	2.81	2.90	2.98	0.17
H(19B)–S(21)	2.72	2.84	2.94	0.22
(b) H···nonhydrogen atom contact distances (Å)				
H(7Be)–C(15)			2.93	
H(7Be)–C(16)			2.57	
H(7Be)–S(17)			3.52	
H(7Be)–S(18)			2.66	
H(8As)–C(15)	2.64	2.72	2.75	0.11
H(8As)–C(16)	2.63	2.74	2.79	0.16
H(8As)–S(17)	2.98	3.04	3.12	0.14
H(8As)–S(18)	2.86	2.99	3.17	0.31
H(10A)–S(6)	2.80	2.82	2.82	0.02
H(17Ae)–C(5)			3.28	
H(17Ae)–C(6)			2.88	
H(17Ae)–S(7)			3.75	
H(17Ae)–S(8)			2.74	
H(18As)–C(5)	2.66	2.75	2.98	0.32
H(18As)–C(6)	2.71	2.80	3.09	0.38
H(18As)–S(7)	2.86	3.00	3.13	0.27
H(18As)–S(8)	3.03	3.03	3.38	0.35
H(19B)–S(16)	2.99	3.22	3.48	0.49
H(20A)–S(16)	2.63	2.64	2.65	0.02
H(20A)–S(3)	3.00	2.99	3.07	0.07
(c) H···H contact distances (Å)				
H(7Be)–H(19A)			2.31	
H(8As)–H(19A)	2.27	2.18	2.13	−0.13
H(9A)–H(17Ae)			2.36	
H(9A)–H(18As)	2.25	2.24	2.04	−0.21
H(17As)–H(20B)	2.17	2.20	2.18	0.01

[a] The e.s.d.'s for the calculated distances are ~0.02–0.03 Å.

[b] Atoms labels with "e" or "s" refer to atoms which are unique to the eclipsed or staggered conformations, respectively. Both conformations were resolved in the 298 K structure. In order to be consistent, all distances, including those for the 15 K neutron structure, are based on calculated hydrogen atom positions for idealized C sp^3 geometry with d_{C-H} = 1.09 Å.

[c] This work.

[d] Ref. (*3*).

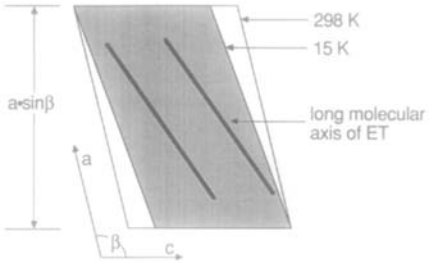

FIG. 6. Schematic drawing of the *ac* plane of the unit cell at 298 and 15 k.

(H(17As)···H(20B)) only occurs in the staggered conformations. This contact remains essentially constant at all temperatures.

Another interesting feature of the κ-$(ET)_2Cu(NCS)_2$ structure is the asymmetry of the H···donor contacts for the eclipsed conformations at 298 K. That is, H(7Be) and H(17Ae) each have one long and one short H···C and H···S contact, whereas the corresponding H(8As) and H(18As) contacts are much more symmetric. It is conceivable that the short contacts in the eclipsed conformations become increasingly unfavorable at low temperatures and are a contributing factor to the adoption of the staggered conformation at 118 K.

The H···anion contact distances (Table IVa) most likely also play a role in the disorder–order transformation. Some of the 118 K distances, such as H(8Bs)···S(22), appear to be anomalously longer than the corresponding 15 and 298 K distances. However, there does not appear to be any systematic variation of the H···anion contact distances that would favor one conformation over the other.

Conclusions

The ET molecules in κ-$(ET)_2Cu(NCS)_2$ exhibit conformational disorder at room temperature. Upon cooling, the molecules order with staggered conformations of the terminal ethylene groups. Examination of

the intermolecular contacts reveals short H···H distances at room temperature due to the staggered conformations. These contacts may be repulsive and the disorder may occur to avoid these unfavorable interactions. At low temperature, the structure orders with staggered conformations which can be accommodated due to the apparent increase in the length of the two shortest H···H distances. The contraction of the unit cell upon cooling is mainly due to a contraction of the spacing between the $Cu(NCS)_2^-$ polymeric anion ribbons. From 298 to 15 K, the perpendicular interlayer spacing $a \cdot \sin \beta$ is constant.

Supplementary Material

Tables of the anisotropic thermal parameters from the 118 K X-ray structure and tables of observed and calculated structure factors for the 118 K X-ray and the 15 K neutron structures are available.[1]

Acknowledgments

Work at Argonne National Laboratory and North Carolina State University is supported by the Office of Basic Energy Sciences, Division of Materials Sciences, U.S. Department of Energy, under Contract W-31-109-ENG-38 and Grant DE-FG05-86ER45259, respectively.

References

1. H. Urayama, H. Yamochi, G. Saito, K. Nozawa, T. Sugano, M. Kinoshita, S. Sato, K. Oshima, A. Kawamoto, and J. Tanaka, *Chem. Lett.*, 55 (1988).
2. S. Gärtner, E. Gogu, I. Heinen, H. J. Keller, T. Klutz, and D. Schweitzer, *Solid State Commun.* **65,** 1531 (1988).
3. K. D. Carlson, U. Geiser, A. M. Kini, H. H. Wang, L. K. Montgomery, W. K. Kwok, M. A. Beno, J. M. Williams, C. S. Cariss, G. W. Crabtree, M.-H. Whangbo, and M. Evain, *Inorg. Chem.* **27,** 965 (1988).
4. J. E. Schirber, E. L. Venturini, A. M. Kini, H. H. Wang, J. R. Whitworth, and J. M. Williams, *Physica C* **152,** 157 (1988).
5. H. Urayama, H. Yamochi, G. Saito, S. Sato, A. Kawamoto, J. Tanaka, T. Mori, Y. Maruyama, and H. Inokuchi, *Chem. Lett.*, 463 (1988).
6. A. J. Schultz, H. H. Wang, J. M. Williams, and A. Filhol, *J. Am. Chem. Soc.* **108,** 7853 (1986).
7. S. Ravy, J. P. Pouget, C. Lenoir, and P. Batail, *Solid State Commun.* **73,** 37 (1990).
8. C. Strouse, "UCLA Crystallographic Program Package" Univ. of California, Los Angeles (1978).
9. A. J. Schultz, *Trans. Am. Crystallogr. Assoc.* **23,** 61 (1987).
10. A. J. Schultz, D. G. Van Derveer, D. W. Parker, and J. E. Baldwin, *Acta Crystallogr. Sect. C* **46,** 276 (1990).
11. W. R. Busing, K. O. Martin, and H. A. Levy, *ORFLS*, Report ORNL-TM-302, Oak Ridge National Laboratory, Oak Ridge, Tennessee, USA (1962).
12. P. J. Becker and P. Coppens, *Acta Crystallogr. Sect. A* **30,** 129 (1974).
13. M.-H. Whangbo, J. M. Williams, A. J. Schultz, T. J. Emge, and M. A. Beno, *J. Am. Chem. Soc.* **109,** 90 (1987).
14. D. Jung, M. Evain, J. J. Novoa, M.-H. Whangbo, M. A. Beno, A. M. Kini, A. J. Schultz, J. M. Williams, and P. J. Nigrey, *Inorg. Chem.* **28,** 4516 (1989).
15. M.-H. Whangbo, J. J. Novoa, D. Jung, J. M. Williams, A. M. Kini, H. H. Wang, U. Geiser, M. A. Beno and K. D. Carlson, *in* "Organic Superconductivity" (V. Kresin, W. L. Little, Eds.), p. 243, Plenum Press, New York (1990).
16. U. Geiser, A. J. Schultz, H. H. Wang, D. M. Watkins, D. L. Stupka, J. M. Williams, J. E. Schirber, D. L. Overmyer, D. Jung, J. J. Novoa, and M.-H. Whangbo, *Physica C* **174,** 475 (1991).

[1] See NAPS document No. 04886 for 22 pages of supplementary materials. Order from ASIS/NAPS, Microfiche Publications, P.O. Box 3513, Grand Central Station, New York, NY 10163. Remit in advance $4.00 for microfiche copy or for photocopy, $7.75 up to 20 pages plus $.30 for each additional page. All orders must be prepaid. Institutions and Organizations may order by purchase order. However, there is a billing and handling charge for this service of $15. Foreign orders add $4.50 for postage and handling, for the first 20 pages, and $1.00 for additional 10 pages of material, $1.50 for postage of any microfiche orders.